Transferable self-welding silver nanowire network as high performance transparent flexible electrode

View the table of contents for this issue, or go to the journal homepage for more

Transferable self-welding silver nanowire network as high performance transparent flexible electrode

Siwei Zhu[1,3]**, Yuan Gao**[1,3]**, Bin Hu**[1]**, Jia Li**[1]**, Jun Su**[1]**, Zhiyong Fan**[2] **and Jun Zhou**[1]

[1] Wuhan National Laboratory for Optoelectronics, and School of Optical and Electronic Information, Huazhong University of Science and Technology, Wuhan 430074, People's Republic of China
[2] Department of Electronic and Computer Engineering, Hong Kong University of Science and Technology, Clear Water Bay, Kowloon, Hong Kong, People's Republic of China

E-mail: jun.zhou@mail.hust.edu.cn

Abstract
High performance transparent electrodes (TEs) with figures-of-merit as high as 471 were assembled using ultralong silver nanowires (Ag NWs). A room-temperature plasma was employed to enhance the conductivity of the Ag NW TEs by simultaneously removing the insulating PVP layer coating on the NWs and welding the junctions tightly. Furthermore, we developed a general way to fabricate TEs regardless of substrate limitations by transferring the as-fabricated Ag NW network onto various substrates directly, and the transmittance can remain as high as 91% with a sheet resistivity of 13 Ω/sq. The highly robust and stable flexible TEs will have broad applications in flexible optoelectronic and electronic devices.

S Online supplementary data available from stacks.iop.org/Nano/24/335202/mmedia

(Some figures may appear in colour only in the online journal)

1. Introduction

Owing to the rapid development of flexible optoelectronic and electronic devices, emerging transparent flexible electrodes based on conducting polymers [1, 2], carbon nanotubes (CNTs) [3–6], graphene [7, 8], metal grids and metallic nanowires (NWs) [9–15] are of increasing importance for applications in these fields, and they can retain the attractive features of commercial indium-doped tin oxide (ITO) transparent electrodes (TEs) such as high electrical conductivity and optical transmittance (T), while also overcoming the shortcomings of ITO TEs such as the scarcity and high cost of indium, and its inherent brittleness [16–18].

To implement practical applications of flexible TEs, the balance between the optimal T and sheet resistivity (R_s) needs to be addressed due to the fact that these two critical parameters typically follow opposite trends. In the pursuit of improving T and simultaneously lowering R_s to achieve a high performance of TEs with $T \geq 90\%$ and $R_s \leq 100$ Ω/sq [19], recently developed Ag NW networks have attracted intense interest due to their excellent T and R_s compared with their conventional counterparts [11, 20–23]. However, they still suffer from issues such as percolation and large inter-nanowire contact resistances [9, 16, 24, 25]. Moreover, the widely used solution-based fabrication techniques have certain requirements for the substrates, for instance, the substrates should be resistant to stress and high temperature [11, 12, 14, 19, 26], possess good wettability for the dispersions [9, 27–29], and the surface geometry should typically be flat for uniform deposition of Ag NWs.

In order to tackle these challenges, in this work we present an optimized approach to synthesize ultralong Ag NWs, which can be assembled into a highly transparent network with low R_s after removing the insulating polymer layer on the Ag NWs and welding the junctions by plasma treatment at room temperature. It is of particular importance

---

[3] These authors contributed equally to the work.
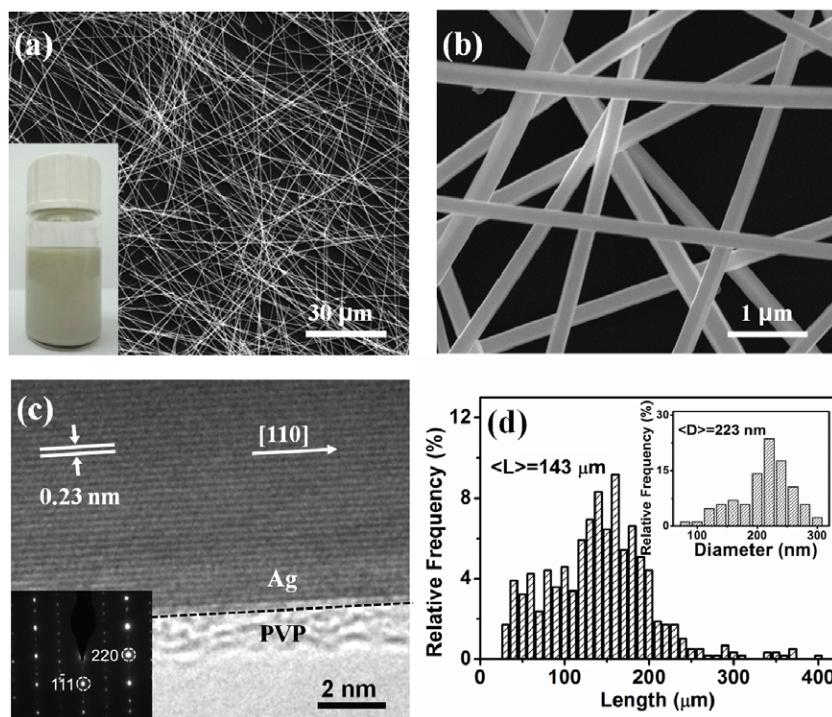
Figure 1. Morphology characterizations of the as-prepared Ag NWs. (a) SEM image of top view of as-prepared Ag NWs on a silicon substrate and their suspensions in alcohol (inset). (b) High-magnification SEM image of Ag NWs. (c) TEM image and SAED pattern (inset) of Ag NWs. (d) Histogram of statistics relating to the length and diameter (inset) of the Ag NWs.

that the as-fabricated robust Ag NW TEs can be transferred to various substrates without severe performance degradation, and T can remain as high as 91% with an R_s only of 13 Ω/sq. These results suggest a generic way to remove the substrate limitations for the fabrication of TEs, and greatly broaden the range of applications of high performance TEs in flexible devices.

2. Experimental procedure

2.1. Synthesis of ultralong Ag NWs

Here, a modified $CuCl_2$-mediated polyol process was used to prepare long Ag NWs [22]. For a typical synthesis, polyvinylpyrrolidone (PVP, 0.26 g, $M_w \sim 1\,300\,000$) and $Cu(NO_3)_2$ (0.6 mg) were added sequentially to a flask and filled with ethylene glycol (80 ml), then the mixture was stirred moderately for 5 min. The solution was then heated at 180 °C for half an hour, and cooled to room temperature in a glass dryer. $AgNO_3$ powder (0.24 g) was then added to the solution with vigorous stirring for 10 min until the powder was fully dissolved. Then the solution was sealed in a bottle and kept at 145 °C for 7 h in an oven. Finally, the obtained products were washed with acetone and alcohol several times, then stored in alcohol for use, as shown in the inset in figure 1(a). The morphology, structure and composition of the samples were probed by a high-resolution field emission scanning electron microscope (SEM, FEI Nova NanoSEM 450) and a high-resolution transmission electron microscope (HRTEM, Tecnai G2 20 U-TWIN).

2.2. The effect of plasma treatment on the properties of Ag NW TEs

The glass substrate was placed onto a hot plate at 92 °C and a few microliters of Ag NW ink was dropped on a Meyer rod with a micropipette. The Meyer rod was either pulled or rolled over the ink along one direction, then an equal volume Ag NW ink was also deposited on the substrate by rolling the Meyer rod along the orthogonal direction. Next, the obtained TE was treated by plasma irradiation for 1 h with a power of 75 W. Increasing the power or introducing oxygen into the plasma could shorten the treatment time, but the Ag NWs will be easily oxidized and the TE will be destroyed. The optical transmittance spectra were recorded using a SHIMADZU UV-2550. In all cases, a glass substrate was used as the reference to measure the regular transmittance. The R_s of the Ag NW TEs was measured by an Agilent U1252 hand-held digital multimeter.

2.3. Procedure for transferable Ag NW TEs

The Ag NW TEs were fabricated on Al-coated polyethylene terephthalate (PET) sheet with a thickness around 100 μm following the aforementioned process. A thin polydimethyl-siloxane (PDMS) layer was coated on the three edges of the network and cured at 80 °C for half an hour; then the edge left without PDMS could release the bubbles produced during the etching reaction. Next, the sample was carefully and slowly inserted in an etching solution of NaOH (2 wt%) and sodium dodecyl benzene sulfonate (0.1 g ml^{-1}) for
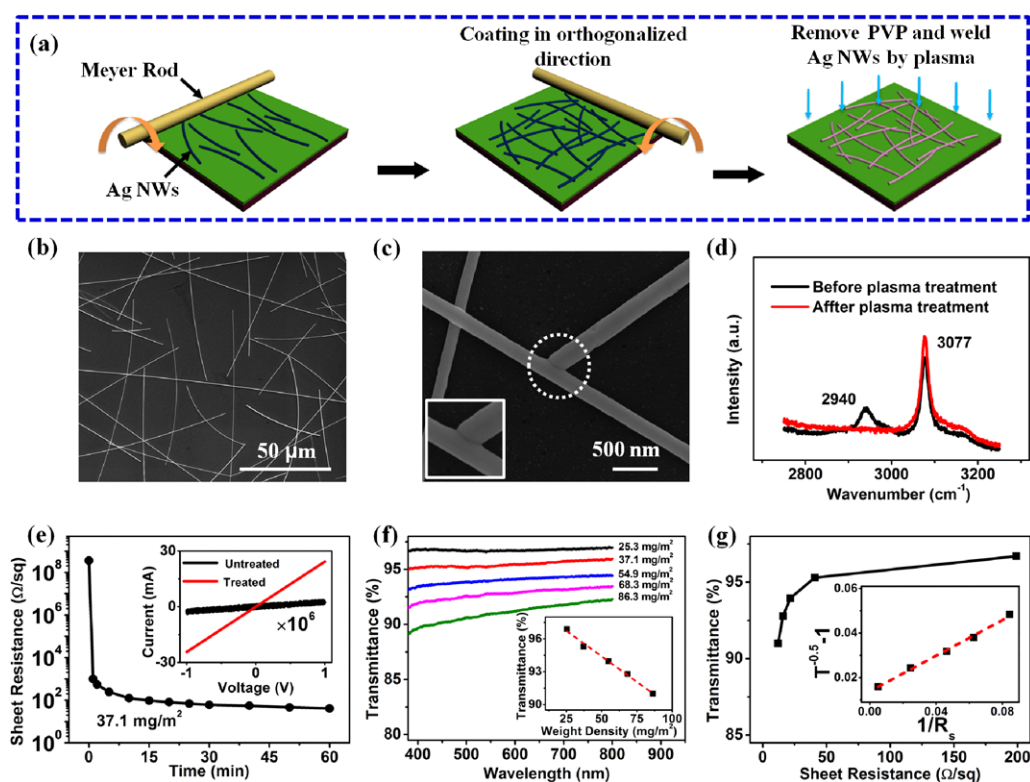
Figure 2. The effect of plasma treatment on the properties of Ag NW TEs. (a) A schematic of the Ag NW TE preparation process. (b) SEM images of welded Ag NWs and (c) zoomed-in view of a welded junction. (d) FT-Raman spectra of a Ag NW TE before and after plasma treatment. (e) Plasma irradiation time versus R_s of Ag NWs (inset: *I–V* curves of the TE before and after plasma treatment). (f) The optical transmittance spectra with different Ag NW weight densities (inset: the relationship between transmittance and Ag NW weight densities). (g) R_s as a function of T with an added linear fitting of $T^{-0.5} - 1$ and $1/R_s$.

8 h until the Al layer was completely dissolved, in which the surfactant can prevent the Ag NWs from adhering to the PET. The etching solution was neutralized by DI water after the Ag NW networks floated up, then target substrates, such as xerox paper, ceramics, clothes or live leaves, were inserted into the DI water and placed below the networks, as illustrated in figure S1 (available at stacks.iop.org/Nano/24/335202/mmedia). Next, the solution was drained slowly until the Ag NW networks laid on the substrates. Finally, the samples were dried at 40 °C.

3. Results and discussion

Ultralong Ag NWs were synthesized through an optimized $CuCl_2$-mediated polyol method. In this optimized process, we used a longer chain PVP to induce the formation of longer Ag NWs than a previous method using short chain PVP [12, 22], as the Ag NW growth mechanism follows the coordination of silver ions with oxygen atoms along the chain of PVP [30]. No stirring during the Ag NW growth process in the oven at 145 °C increases the possibility of bonding of the formed seeds and silver atoms [31]. The lower reaction temperature (145 °C) adopted and the longer reaction time (7 h) decreased the nucleation rate and left more silver precursor available to increase the growth length [14]. Finally, $Cu(NO_3)_2$ was used as an additive instead of $CuCl_2$

(see figure S2 available at stacks.iop.org/Nano/24/335202/mmedia). Figures 1(a) and (b) show SEM images of randomly oriented Ag NWs produced by dripping a drop of Ag NW ink (inset in figure 1(a)) on the Si substrate. The smooth Ag NWs possess high crystallinity with the growth direction shown in the TEM image in figure 1(c) and the inserted selected area electron diffraction (SAED) pattern. A thin amorphous PVP layer coating on the surface could be clearly observed, which is consistent with previous reports [32, 33]. The statistics of the length and diameter distributions of Ag NWs given in figure 1(d) show that the average diameter is ∼223 nm (inset in figure 1(d)), and it is worth noting that the average length up to ∼ 143 μm is much longer than those grown by a successive multistep growth (SMG) method [12]. Longer NWs will result in a lower R_s and better T and mechanical flexibility.

The Ag NWs were first coated on the glass substrate using an improved Meyer rod method for TE fabrication, as illustrated in figure 2(a). We found rolling the Meyer rod along two orthogonal directions enabled the more efficient interconnection of Ag NWs (figure 2(b)) [34]. Compared with single-direction rolling (figure S3(a) available at stacks.iop.org/Nano/24/335202/mmedia), all of the quasi-parallel NWs could be well bridged (figures S3(b) and (c) available at stacks.iop.org/Nano/24/335202/mmedia), implying more pathways formed in the network for electron transport, and leading to improved robustness of the TEs as well.

It has been reported that the residual insulating PVP layer coating on the Ag NWs that we observed in the TEM image would drastically affect the conductivity of the TEs [16, 24, 32], thus many approaches have been used to remove the PVP layer [12, 14, 24, 25]. In our study, we employed a room-temperature plasma to achieve this goal [35], which is a more advantageous way due to the fact that it causes hardly any damage to the flexible polymer substrates as compared with optothermal annealing using a broadband lamp [27]. Another great advantage is that it can eliminate the PVP layer on the Ag NWs completely, not just at the junctions between two neighboring Ag NWs (figure S4 available at stacks.iop.org/Nano/24/335202/mmedia). This feature is highly attractive for applications of the Ag NW TEs as the top electrodes in solar cells. The effect of plasma treatment on the PVP layer was verified by an FT-Raman spectrometer (figure 2(d)), in which the peak of the asymmetric stretching vibration of CH_2 in the skeletal chain of PVP that is located at 2940 cm^{-1} vanished entirely after 1 h irradiation [32]. The FT-Raman spectra of Ag NW TEs treated with plasma for 1–5 min are presented in figure S5 (available at stacks.iop.org/Nano/24/335202/mmedia). In addition, plasma irradiation was also capable of inducing self-welding of the Ag NWs, as we can see clearly in figure 2(c) and figure S6 (available at stacks.iop.org/Nano/24/335202/mmedia), implying that the contact resistances of Ag NWs junctions could be reduced. The welding behavior could improve the conductivity of the network as well, and significantly reinforce the mechanical robustness of transferable TEs. Figure 2(e) shows the effect of plasma treatment time on the value of R_s of Ag NW TEs quantitatively using a sample with a weight density of around 37.1 mg m^{-2}. In the first minute, the value of R_s decreased dramatically owing to the rapid removal of insulating PVP on the NWs, and the following gentle reduction of the curve indicates the residual PVP was completely cleaned with the junctions welded together. Finally, R_s was reduced by six orders of magnitude and lowered to tens of ohms. As shown in figure 2(f), the corresponding optical transmittance spectra was also investigated by measuring the typical T of five samples with different weight densities. We can see that T was inversely proportional to the weight density at a wavelength of 550 nm, but still retained a high value even under a large weight density. The flat curves without absorption peaks confirm their excellent transparent properties across the visible range.

As a non-continuous network, equation (1) was used to link T to the dimensions of the NWs [14]:

$$T = 1 - 2aNLr \tag{1}$$

where a is a fitting parameter accounting for the diameter- and wavelength-dependent optical properties of the NWs, L and r are the length and radius of the NWs respectively, and N, the number density of Ag NWs (number of NWs per square meter), can be expressed as:

$$N = m_s/(\pi r^2 L \rho) \tag{2}$$

where m_s is the weight density of Ag NWs (weight of NWs per square meter) and ρ is the density of silver. Combining equations (1) and (2), T can be expressed as:

$$T = 1 - 2a/(\pi r \rho)m_s. \tag{3}$$

We can observe the inverse linear relationships between T and the radius of the Ag NWs when m_s and a are constant. Using the fitting formula $T = b - (2a/\pi r \rho)m_s$, a and b can be found to be 1.73 and 99.1% respectively, with $R^2 = 0.991$ and Pearson's $r = -0.997$ (inset in figure 2(f)). The value of a is related to the scattering efficiency of the Ag NWs [14], and the value of b closely approximates the theoretical value of 100%, which originates from an accurate calculation of m_s [24]. Since the measurement of T was generally accurate, the experimental error came mainly from the measurement of m_s. The relationship between the experimentally determined R_s and the normalized number density $N/N_c - 1$ was also plotted to compare our results with the theoretical prediction (figure S7 available at stacks.iop.org/Nano/24/335202/mmedia), where N_c is the critical number density [14]. The conductivity exponent was extracted as $t = 1.34$, which is in good agreement with the theoretical value and reported result for a 2D NW network [14, 36]. This fact implied that the junction resistance of Ag NWs was very close to the body resistance [36] and proved that the Ag NWs had been welded tightly with a very low contact resistance after plasma treatment.

To evaluate the performance of Ag NW TEs as an applicable electrode, a relationship between T and R_s in the percolation regime is proposed in figure 2(g). The ratio of DC conductivity (σ_{dc}) to optical conductivity (σ_{op}) is usually used as a figure-of-merit (FOM) to evaluate the quality of TEs, and a higher FOM leads to a higher T with a lower R_s. According to equation (4) [17],

$$T = \left(1 + \frac{188.5}{R_s}\frac{\sigma_{op}}{\sigma_{dc}}\right)^{-2}. \tag{4}$$

The FOM of our sample was calculated to be as high as 471 (inset in figure 2(g)), which exceeded many reported results, such as 459 for Ag NWs [12], 100 for short Cu NWs [13], 125 for long Cu NWs [37], 102 for graphene [8] and 24 for single-wall CNTs [38]. This high FOM of the Ag NW network mostly results from the long length of the Ag NWs. According to the simulations of the conductivity in stick percolation [12–15, 19, 36], longer NWs required a much lower NW number density for percolation than short NWs. Therefore, given the constant transmittance and diameter, a network of longer NWs possesses a lower sheet resistance. In addition, a network of longer NWs has fewer junctions and thus a lower junction resistance than a network of short NWs. Moreover, plasma treatment at room temperature can further enhance the performance of the network. Therefore, we believe these two factors together contributed to the high FOM of the Ag NW TE.

In order to transfer the Ag NW TE onto other substrates, a self-sacrificial substrate of Al-coated PET sheet was used instead of glass, following the same process illustrated in figure 2(a). The ultrathin freestanding Ag NW network fixed by a thin layer of PDMS frame could float on the etching solution without cracking, wrinkling or scattering after
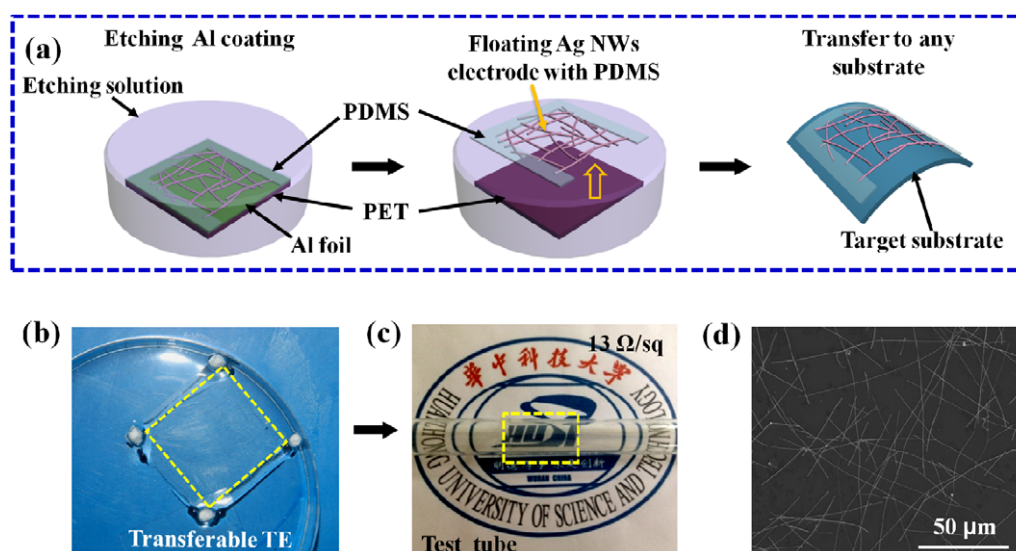
Figure 3. (a) Schematic of the Ag NW TE transfer process. (b) Optical photograph of a transferable Ag NW TE floating on the surface of the solution. (c) Ag NW TE transferred onto the test tube with a sheet resistance of about 13 Ω/sq and (d) the corresponding SEM image. (The TE is marked by the dashed box.)

completely dissolving the Al layer, as shown in figures 3(a) and (b), and the original properties of the Ag NW TEs could be maintained.

Various substrates, including a hydrophobic bamboo leaf, flexible PET, ceramic plate, xerox paper, and rough cloth were chosen for the transfer of the as-prepared TEs, with R_s values of about 19 Ω/sq, 16 Ω/sq, 12 Ω/sq, 25 Ω/sq, and 233 Ω/sq, respectively (figure S8 available at stacks.iop.org/Nano/24/335202/mmedia). The freestanding TEs can also stick on a curved surface, such as the test tube shown in figure 3(c) with a resistance of 13 Ω/sq, which cannot be achieved by previously reported methods [3, 27, 28, 39, 40]. In most cases, the freestanding Ag NW electrode maintained a good transmittance after transfer ($T = 91\%$, $R_s = 13$ Ω/sq) (figure S9 available at stacks.iop.org/Nano/24/335202/mmedia); values better than other carbon-based transferable electrodes such as graphene ($T = 80\%$, $R_s = 280$ Ω/sq) [7] and CNTs ($T = 85\%$, $R_s = 60$ Ω/sq) [5].

The flexibility and stability of the Ag NW TEs are two important properties for long-life flexible electronics. The stability of the Ag NW TE transferred onto xerox paper under four different bending curvatures was monitored at a fixed voltage of 0.3 V (figure 4(a)), and each bending curvature was maintained for 60 s, as shown in the insets. We found the current was very stable and had no apparent change even under a bending amplitude of 12 mm, revealing that the conductance of the Ag NW electrode was hardly affected by bending stress; similar behavior was also observed during the recovery process, indicating its excellent reversibility. The long-term stability was studied by fixing one end of the Ag NW electrode on a resonator to bend and release it repetitively (inset in figure 4(b)). After 10 000 bending cycles with a 2 Hz bending frequency and a 2 mm amplitude, there was no observable R_s change. The exhibited superior mechanical reliability of the Ag NW flexible TE can be attributed to the

electrode network that was built by ultralong Ag NWs which could withstand more deformation than a network consisting of shorter NWs [12, 41]. Moreover, the actual application of a Ag NW TE as a conductor, shown in figure 4(c), demonstrated operation of LEDs, and the *I–V* curve of a flexible Ag NW TE on paper overlapped with that using a normal copper conductor, indicating the promising potential of Ag NW electrodes to replace conventional bulk metal electrodes.

4. Conclusion

In summary, we fabricated flexible, transparent electrodes by means of an optimized Meyer rod coating method using an ink with ultralong Ag NWs. The employed plasma treatment can effectively enhance the conductivity of the Ag NW TEs by simultaneously removing the insulating PVP layer coating on the NWs and welding the junctions tightly. The relationship between T and the weight density was studied in detail, and an excellent performance of the Ag NW TEs was found, with a FOM as high as 471. More importantly, we successfully demonstrated an approach to transfer Ag NW TEs onto various substrates without severe performance degradation. We believe the obtained highly robust and stable flexible TEs have broad applications in flexible optoelectronic and electronic devices, and this low-cost efficient process can be used as a generic method for the fabrication of other transferable metal NW electrodes.

Acknowledgments
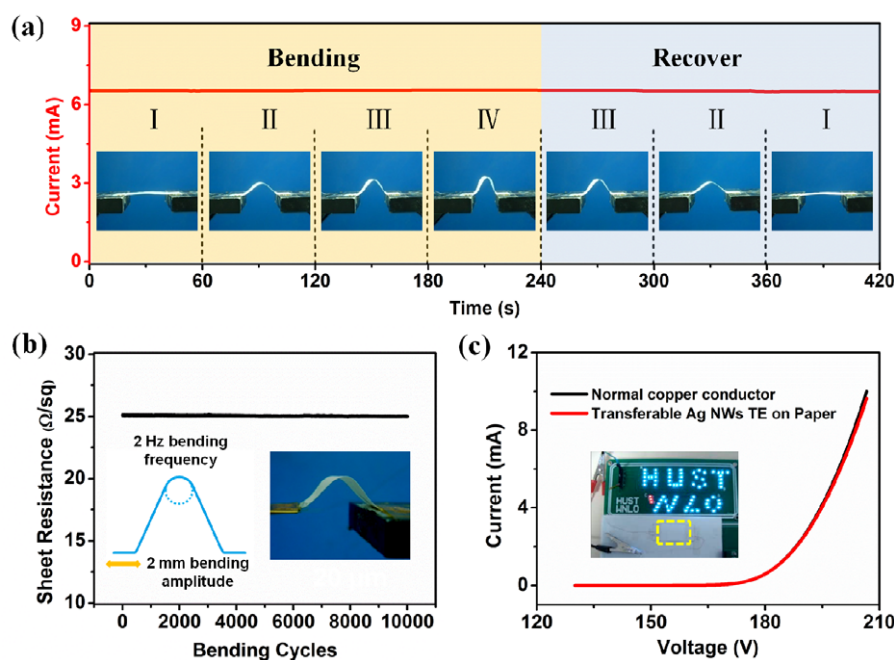
Figure 4. The mechanical properties of a Ag NW TE transferred onto xerox paper and a real application as a conductor. (a) *I–t* curve of a Ag NW TE bent with different curvatures under a constant voltage of 0.3 V. The insets labeled I–IV demonstrate the four bending states. (b) The measurement of R_s during 10 000 bending cycles with a 2 mm bending amplitude. Insets show the bending state of the flexible conductor. (c) Operation of the LED display using a Ag NW TE instead of a normal copper conductor.

References

[1] Tran H D, Li D and Kaner R B 2009 One-dimensional conducting polymer nanostructures: bulk synthesis and applications *Adv. Mater.* **21** 1487–99

[2] Yin Z and Zheng Q 2012 Controlled synthesis and energy applications of one-dimensional conducting polymer nanostructures: an overview *Adv. Energy Mater.* **2** 179–218

[3] Wu Z *et al* 2004 Transparent, conductive carbon nanotube films *Science* **305** 1273–6

[4] Hu L, Hecht D S and Grüner G 2004 Percolation in transparent and conducting carbon nanotube networks *Nano Lett.* **4** 2513–7

[5] Nasibulin A G *et al* 2011 Multifunctional free-standing single-walled carbon nanotube films *ACS Nano* **5** 3214–21

[6] Zhang D, Wang R, Wen M, Weng D, Cui X, Sun J, Li H and Lu Y 2012 Synthesis of ultralong copper nanowires for high-performance transparent electrodes *J. Am. Chem. Soc.* **134** 14283–6

[7] Kim K S, Zhao Y, Jang H, Lee S Y, Kim J M, Ahn J H, Kim P, Choi J Y and Hong B H 2009 Large-scale pattern growth of graphene films for stretchable transparent electrodes *Nature* **457** 706–10

[8] Bae S *et al* 2010 Roll-to-roll production of 30-inch graphene films for transparent electrodes *Nature Nano* **5** 574–8

[9] Cui Y, Hu L B, Kim H S, Lee J Y and Peumans P 2010 Scalable coating and properties of transparent, flexible, silver nanowire electrodes *ACS Nano* **4** 2955–63

[10] Rathmell A R, Nguyen M, Chi M and Wiley B J 2012 Synthesis of oxidation-resistant cupronickel nanowires for transparent conducting nanowire networks *Nano Lett.* **12** 3193–9

[11] De S, Higgins T M, Lyons P E, Doherty E M, Nirmalraj P N, Blau W J, Boland J J and Coleman J N 2009 Silver nanowire networks as flexible, transparent, conducting films: extremely high dc to optical conductivity ratios *ACS Nano* **3** 1767–74

[12] Lee J, Lee P, Lee H, Lee D, Lee S S and Ko S H 2012 Very long Ag nanowire synthesis and its application in a highly transparent, conductive and flexible metal electrode touch panel *Nanoscale* **4** 6408–14

[13] Rathmell A R and Wiley B J 2011 The synthesis and coating of long, thin copper nanowires to make flexible, transparent conducting films on plastic substrates *Adv. Mater.* **23** 4798–803

[14] Bergin S M, Chen Y H, Rathmell A R, Charbonneau P, Li Z Y and Wiley B J 2012 The effect of nanowire length and diameter on the properties of transparent, conducting nanowire films *Nanoscale* **4** 1996–2004

[15] Madaria A R, Kumar A and Zhou C 2011 Large scale, highly conductive and patterned transparent films of silver nanowires on arbitrary substrates and their application in touch screens *Nanotechnology* **22** 245201

[16] Hecht D S, Hu L and Irvin G 2011 Emerging transparent electrodes based on thin films of carbon nanotubes, graphene, and metallic nanostructures *Adv. Mater.* **23** 1482–513

[17] Hecht D S and Kaner R B 2011 Solution-processed transparent electrodes *MRS Bull.* **36** 749–55

[18] Ellmer K 2012 Past achievements and future challenges in the development of optically transparent electrodes *Nature Photon.* **6** 809–17

[19] Sorel S, Lyons P E, De S, Dickerson J C and Coleman J N 2012 The dependence of the optoelectrical properties of silver nanowire networks on nanowire length and diameter *Nanotechnology* **23** 185201

[20] Hu L, Wu H and Cui Y 2011 Metal nanogrids, nanowires, and nanofibers for transparent electrodes *MRS Bull.* **36** 760–5

[21] Xia Y N, Sun Y G, Yin Y D, Mayers B T and Herricks T 2002 Uniform silver nanowires synthesis by reducing AgNO$_3$ with ethylene glycol in the presence of seeds and poly(vinyl pyrrolidone) *Chem. Mater.* **14** 4736–45

[22] Korte K E, Skrabalak S E and Xia Y 2008 Rapid synthesis of silver nanowires through a CuCl- or CuCl$_2$-mediated polyol process *J. Mater. Chem.* **18** 437–41

[23] Wiley B, Sun Y and Xia Y 2007 Synthesis of silver nanostructures with controlled shapes and properties *Acc. Chem. Res.* **40** 1067–76

[24] Lee J-Y, Connor S T, Cui Y and Peumans P 2008 Solution-processed metal nanowire mesh transparent electrodes *Nano Lett.* **8** 689–92

[25] Garnett E C, Cai W, Cha J J, Mahmood F, Connor S T, Greyson Christoforo M, Cui Y, McGehee M D and Brongersma M L 2012 Self-limited plasmonic welding of silver nanowire junctions *Nature Mater.* **11** 241–9

[26] De S *et al* 2009 Transparent, flexible, and highly conductive thin films based on polymer–nanotube composites *ACS Nano* **3** 714–20

[27] Kim T, Kim Y W, Lee H S, Kim H, Yang W S and Suh K S 2012 Uniformly interconnected silver-nanowire networks for transparent film heaters *Adv. Funct. Mater.* **23** 1250–5

[28] Yu Z, Zhang Q, Li L, Chen Q, Niu X, Liu J and Pei Q 2011 Highly flexible silver nanowire electrodes for shape-memory polymer light-emitting diodes *Adv. Mater.* **23** 664–8

[29] Hu L *et al* 2013 Transparent and conductive paper from nanocellulose fibers *Energy Environ. Sci.* **6** 513–8

[30] Zhu J-J, Kan C-X, Wan J-G, Han M and Wang G-H 2011 High-yield synthesis of uniform Ag nanowires with high aspect ratios by introducing the long-chain PVP in an improved polyol process *J. Nanomater.* **2011** 1–7

[31] Coskun S, Aksoy B and Unalan H E 2011 Polyol synthesis of silver nanowires: an extensive parametric study *Cryst. Growth Des.* **11** 4963–9

[32] Gao Y *et al* 2004 Evidence for the monolayer assembly of poly(vinylpyrrolidone) on the surfaces of silver nanowires *J. Phys. Chem.* B **108** 12877–81

[33] Soejima T and Kimizuka N 2009 One-pot room-temperature synthesis of single-crystalline gold nanocorolla in water *J. Am. Chem. Soc.* **131** 14407–12

[34] Li J, Zhang Z-B, Ostling M and Zhang S-L 2008 Improved electrical performance of carbon nanotube thin film transistors by utilizing composite networks *Appl. Phys. Lett.* **92** 133103

[35] Demming A 2013 Plasmas and plasmons: links in nanosilver *Nanotechnology* **24** 090201

[36] Li J and Zhang S-L 2010 Conductivity exponents in stick percolation *Phys. Rev.* E **81** 021120

[37] Zhang D, Wang R, Wen M, Weng D, Cui X, Sun J, Li H and Lu Y 2012 Synthesis of ultralong copper nanowires for high-performance transparent electrodes *J. Am. Chem. Soc.* **134** 14283–6

[38] Mirri F, Ma A W K, Hsu T T, Behabtu N, Eichmann S L, Young C C, Tsentalovich D E and Pasquali M 2012 High-performance carbon nanotube transparent conductive films by scalable dip coating *ACS Nano* **6** 9737–44

[39] Akter T and Kim W S 2012 Reversibly stretchable transparent conductive coatings of spray-deposited silver nanowires *ACS Appl. Mater. Int.* **4** 1855–9

[40] Leem D-S, Edwards A, Faist M, Nelson J, Bradley D D C and de Mello J C 2011 Efficient organic solar cells with solution-processed silver nanowire electrodes *Adv. Mater.* **23** 4371–5

[41] Yang C, Gu H, Lin W, Yuen M M, Wong C P, Xiong M and Gao B 2011 Silver nanowires: From scalable synthesis to recyclable foldable electronics *Adv. Mater.* **23** 3052–6